Synthesis and electrochemical characterisation of some long chain 1,4,8,11,15,18,22,25-octa-alkylated metal-free and zinc phthalocyanines possessing discotic liquid crystalline properties

Jannie C. Swarts,*[a] Ernie H. G. Langner,[a] Nina Krokeide-Hove[b] and Michael J. Cook*[b]

[a]Department of Chemistry, University of the Orange Free State, Bloemfontein 9300, Republic of South Africa. E-mail: swartsjc@cem.nw.uovs.ac.za
[b]School of Chemical Sciences, University of East Anglia, Norwich NR4 7TJ, UK

A series of long chain (C_{10}, C_{12}, C_{15} and C_{18}) 3,6-dialkylated phthalonitriles, prepared in 4 steps from thiophene, have been converted into the title phthalocyanines as metal-free and zinc derivatives. The symmetric macrocycles were characterised using ^{1}H NMR, MALDI-TOF ms and solution phase electronic (UV-VIS) spectroscopy. Four ring-based redox processes for the metal-free macrocycles possessing shorter alkyl substituents could be identified in the potential range −1.8 to 1.2 V vs. Ag/Ag$^+$ in dichloromethane or 1,2-dichloroethane. Reversibility became poorer with an increase in chain length of the eight alkyl substituents. The redox processes of the zinc complexes were not as well defined as those of the metal-free phthalocyanines. All compounds exhibited discotic thermotropic liquid crystal behaviour, which was studied using polarised optical microscopy and differential scanning calorimetry (DSC). Up to three different mesophases were detected. The zinc derivatives showed liquid crystalline behaviour at much higher temperatures than the metal-free compounds. The metal-free and zinc phthalocyanines with C_{12} chains had the lowest crystalline to discotic liquid crystalline mesophase transition temperatures. Variable temperature UV-VIS spectra of thin films (ca. 1000 Å thick) of the title compounds cast on glass were obtained for the compounds in the crystalline, meso- and isotropic liquid phase. The spectrum of a thin film of the isotropic liquid resembled the spectrum obtained from a solution of the same compound.

Introduction

Phthalocyanines have been investigated inter alia for applications such as dyestuffs,[1] blue and green pigments,[2] chemical sensors,[1,3] photodynamic cancer drugs,[4] non-linear optical materials,[5] converters of visible light energy (from solar radiation) into various other forms of energy including chemical[6] and electrical energy,[7] catalysts in a variety of chemical reactions including hydrogenation of multiple bonds[8] and oxidation of thiols,[9] and as liquid crystals.[10]

One of our groups has reported wide ranging investigations of non-peripherally substituted 1,4,8,11,15,18,22,25-octakis-alkylphthalocyanines. These have been obtained as metal-free, copper, cobalt, nickel[11] and zinc[12] derivatives and homologous series have been synthesized in which the length of the alkyl chains has been varied from methyl through to decyl. The compounds have proved of interest for a number of reasons. Examples form unusually well ordered spin coated films,[11,13] those with longer chains form liquid crystal phases,[11] a compound within its mesophase has shown rapid response and recovery times in gas sensing studies[14] and zinc derivatives show beneficial properties in the photodynamic therapy of cancer.[15] Structure–behaviour relationships have been established particularly in the area of columnar mesophase formation and the role of chain length and metal ion on phase transition temperatures and mesophase range has been established.[11] In each series liquid crystallinity is exhibited by compounds with C_6–C_{10} chains. The series of zinc derivatives is unique in that the C_5 chain proved to be the limiting chain length which supports mesophase behaviour. Zinc also has a beneficial effect in stabilising the mesophases, enhancing the temperature range over which liquid crystalline properties could be detected. The Zn–$C_{10}H_{21}$ derivative, for example, is

liquid crystalline between 89.6 and 225.1 °C. In contrast the temperature range in which the corresponding nickel derivative is liquid crystalline is 64.2–135.9 °C.[11]

Investigations into the solution phase behaviour of the zinc series showed that solubility and aggregation in cyclohexane is critically affected by chain length. ZnPc–C_{10} (Pc = phthalocyanine) shows departure[16] from the Beer–Lambert law at 1.5×10^{-4} mol dm^{-3} in contrast to the ZnPc–C_5 through ZnPc–C_9 derivatives which showed departures between ca. 1×10^{-5} and 4×10^{-5} mol dm^{-3}. Non-aggregating phthalocyanines are of interest in luminescence studies because quenching is minimised and have been identified as having potential importance in photodynamic therapy.

The present paper describes the synthesis of novel longer chain homologues of the zinc series and of the metal-free series from which they were obtained. These have enabled us to investigate the effect of the longer chains on mesophase behaviour, thin film properties and solution phase properties. The potential for encapsulating the phthalocyanine core within the compounds' own side chains becomes a real possibility and this has been explored in the solution phase by an electrochemical investigation, the first of its kind to be applied to any of the octa-alkyl phthalocyanine derivatives investigated hitherto.

Results and discussion

Synthesis and characterisation

Phthalocyanines were prepared according to Scheme 1, and results are summarised in Tables 1 and 2. We report here optimised conditions for techniques described in earlier work[12] as well as a new synthetic approach to the oxidation of long

DOI: 10.1039/b006123i
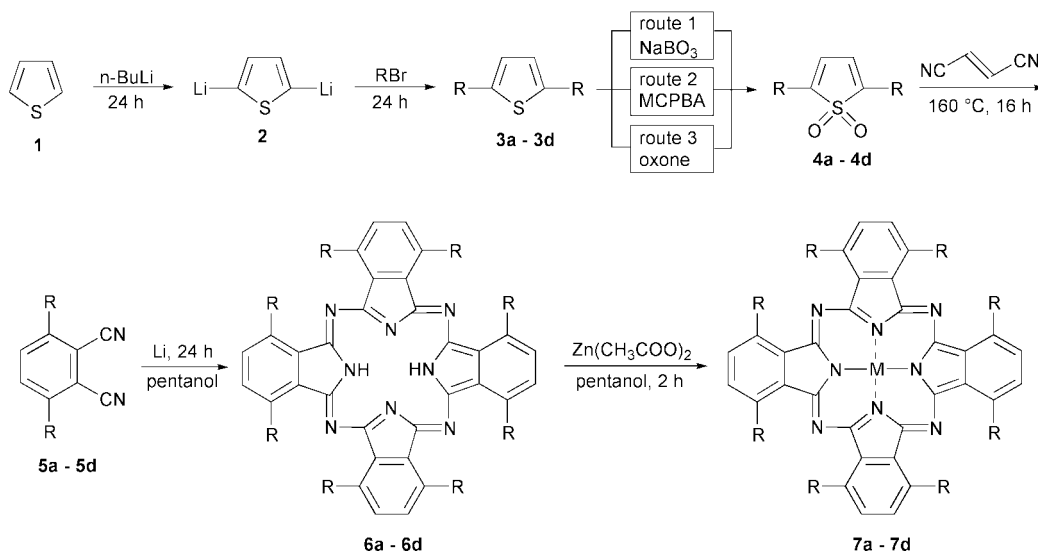
Scheme 1 Syntheses of phthalocyanines **6** and **7**. **a**: R = (CH₂)₉CH₃, **b**: R = (CH₂)₁₁CH₃, **c**: R = (CH₂)₁₄CH₃, **d**: R = (CH₂)₁₇CH₃. In route 3, oxone was reacted *in situ* with acetone to yield the effective oxidant, dimethyldioxirane. Conversion of **4** to **5** is accompanied by SO₂ elimination and dehydrogenation. MCPBA = *m*-chloroperoxybenzoic acid.

chain dialkylated thiophenes to the corresponding dioxides. Lithiation of thiophene, **1**, to give the dilithiated product, **2**, followed by alkylation of the intermediate to give **3** were high yielding (>80%) reactions, even for long linear alkyl chains containing up to 18 carbon atoms. Shorter reaction times than ∼24 h lowered the yields for long chain dialkylations. Oxidation of the 2,5-dialkylthiophene derivatives **3** to the corresponding 2,5-dialkylthiophene 1,1-dioxide **4** became more difficult on increasing the length of the alkyl chains. Potassium permanganate failed to oxidise the derivatised thiophenes to the corresponding oxides. Oxidation with sodium perborate[17] proved to be only effective for linear alkyl substituents containing up to 10 carbon atoms.[12] For R = (CH₂)₁₁CH₃, yields with this oxidant fell from ∼46% (for the C₁₀H₂₁ derivative) to 17%. No thiophene dioxide was isolated for the oxidation of **3** with R = (CH₂)₁₇CH₃. The poor solubility of the dialkylated thiophenes, **3**, with the longer alkyl chains in the solvent of choice for sodium perborate-induced oxidations, glacial acetic acid, probably contributes much to the observed decrease in yields. When oxidation of series **3** was performed with *m*-chloroperoxybenzoic acid, MCPBA, in dichloromethane[18] the yield of 2,5-bis(dodecyl)thiophene 1,1-dioxide was increased to 41% after 18 hours, but yields for the C₁₈H₃₇ derivative remained unsatisfactory. However, when oxidation of series **3** was performed with dimethyldioxirane,[19] near quantitative oxidation was observed for all dialkylated

thiophenes *provided stirring of the heterogeneous reaction mixture was efficient*. We found that dimethyldioxirane need not be isolated by distillation prior to thiophene oxidation as described by Miyahara and co-workers.[20] In our modification of Miyahara's method,[20] dimethyldioxirane was generated *in situ* in the reaction mixture already containing the thiophene that is to be oxidised by reacting acetone with Oxone® (2KHSO₅·KHSO₄·K₂SO₄) in the presence of potassium hydrogen carbonate. The concentration of the generated dimethyldioxirane varies, but good results in our one-pot procedure were obtained by assuming a concentration of 0.08 mol dm⁻³. This concentration is the average of concentrations found when the generated dimethyldioxirane is distilled from sulfide-free generation vessels as were reported by various other researchers.[20]

The Diels–Alder condensation between fumaronitrile and the thiophene 1,1-dioxides, **4**, followed by subsequent *in situ* SO₂ extrusion and dehydrogenation of the intermediate to give the phthalonitrile derivatives, **5**, proceeded simultaneously in a sealed glass tube over 16 hours at 160 °C in the presence of a minimal quantity of chloroform (1.0–1.5 cm³ for 6.5 mmol fumaronitrile, the volume needed to wash the reactants through the nozzle of the tube). Larger quantities of chloroform reduced the yield of the desired phthalonitrile dramatically. Cyclisation of the phthalonitriles in refluxing pentanol in the presence of lithium metal to give the

Table 1 Preparation and characterisation of 2,5-dialkylthiophenes (**3**), 2,5-dialkylthiophene 1,1-dioxides (**4**), *via* dimethyldioxirane oxidation, and 3,6-dialkylphthalonitriles (**5**). See Scheme 1

| Compound | Yield(%) | Mp/°C | Formula | % Found(requires) | | | δ(¹H), 270 MHz, CDCl₃ |
				C	H	S	
3a	70	166ᵃ	C₂₄H₄₄S	79.2(79.0)	12.3(12.2)	8.7(8.8)	0.90 (t, 6 H), 1.3 (m, 28 H), 1.64 (m, 4 H), 2.71 (t, 4 H), 6.48 (s, 2 H)
3b	42	25(217ᵃ)	C₂₈H₅₂S	79.9(79.9)	12.4(12.5)	7.6(7.6)	0.90 (t, 6 H), 1.3 (m, 38 H), 1.65 (m, 4 H), 2.73 (t, 4 H), 6.53 (s, 2 H)
3c	80	43	C₃₄H₆₄S	80.4(80.8)	12.7(12.8)	6.1(6.4)	0.90 (t, 6 H), 1.3 (m, 48 H), 1.68 (m, 4 H), 2.78 (t, 4 H), 6.58 (s, 2 H)
3d	94	56	C₄₀H₇₆S	81.6(81.6)	13.0(13.0)	5.5(5.4)	0.88 (t, 6 H), 1.3 (m, 60 H), 1.63 (m, 4 H), 2.76 (t, 4 H), 6.54 (s, 4 H)
4a	48ᵇ	61–62	C₂₄H₄₄SO₂	72.6(72.7)	10.9(11.2)	7.8(8.1)	0.90 (t, 6 H), 1.3 (m, 28 H), 1.64 (m, 4 H), 2.50 (t, 4 H), 6.22 (s, 2 H)
4b	98	73	C₂₈H₅₂SO₂	73.8(74.2)	11.5(11.6)	6.8(7.1)	0.90 (t, 6 H), 1.3 (m, 36 H), 1.64 (m, 4 H), 2.49 (t, 4 H), 6.25 (s, 2 H)
4c	95	79	C₃₄H₆₄SO₂	75.9(76.0)	12.0(12.0)	6.0(6.0)	0.90 (t, 6 H), 1.3 (m, 48 H), 1.62 (m, 4 H), 2.48 (t, 4 H), 6.25 (s, 2 H)
4d	85	88	C₄₀H₇₆SO₂	77.4(77.4)	12.4(12.3)	4.7(5.1)	0.90 (t, 6 H), 1.28 (m, 60 H), 1.62 (m, 4 H), 2.47 (t, 4 H), 6.23 (s, 2 H)
5a	25	70	C₂₈H₄₄N₂	82.1(82.3)	11.2(10.9)	6.8(6.9)ᶜ	0.90 (t, 6 H), 1.28 (m, 28 H), 1.64 (m, 4 H), 2.86 (t, 4 H), 7.50 (s, 2 H)
5b	27	75	C₃₂H₅₂N₂	82.8(82.7)	11.1(11.2)	6.1(6.0)ᶜ	0.90 (t, 6 H), 1.3 (m, 38 H), 1.63 (m, 4 H), 2.85 (t, 4 H), 7.48 (s, 2 H)
5c	26	79	C₃₈H₆₄N₂	83.4(83.1)	11.7(11.8)	4.9(5.1)ᶜ	0.90 (t, 6 H), 1.3 (m, 48 H), 1.63 (m, 4 H), 2.86 (t, 4 H), 7.48 (s, 2 H)
5d	27	82	C₄₄H₇₆N₂	83.6(83.5)	12.0(12.1)	4.2(4.4)ᶜ	0.89 (t, 6 H), 1.3 (m, 60 H), 1.63 (m, 4 H), 2.83 (t, 4 H), 7.47 (s, 2 H)

ᵃBp at 0.1 torr (= 13.33 Pa). ᵇOxidised with MCPBA. ᶜNitrogen content.

Table 2 Preparation and characterisation of metal-free (6) and zinc-1,4,8,11,15,18,22,25-octa-alkylphthalocyanines (7). See Scheme 1

Compound, Yield Formula	% Found(requires) C	H	N	Transition temp./°C[a]	δ (¹H), 270 MHz[b] $[\lambda_{max}/nm\ (10^{-5}\varepsilon),$ Q-band[i]; $\{\lambda_{max}/nm\ (10^{-5}\varepsilon),$ Soret band[c]}]
6a, 40% $C_{112}H_{178}N_8$	82.2 (82.2)	11.2 (11.0)	6.9 (6.9)	77.5(K→D_1;80)	[d]0.9 (t, 24 H), 1.3 (m, 82 H), 1.55 (m, 16 H), 1.81 (m, 16 H), 2.41 (m, 16 H), 4.80 (t, 16 H), 7.8 (s, 8 H); [730 (0.88), 700 (0.65), 664 (0.24), 635 (0.17)]; {355 (0.36), 310 (0.33)}
6b, 21% $C_{128}H_{210}N_8$	82.2 (82.6)	11.2 (11.4)	5.6 (6.0)	133(D_1→I ; 8.8); 59.2(K→D_3;35); 77.8(D_3→D_1; —); 115.5(D_1→I; 26)	[d]0.9 (t, 24 H), 1.25 (m, 112 H), 1.5 (m, 16 H), 1.85 (m, 16 H), 2.38 (m, 16 H), 4.77 (t, 16 H), 7.95 (s, 8 H); [728 (1.04), 696 (0.89), 660 (0.33), 628 (0.24); {354 (0.49), 305 (0.42)}
6c, 19% $C_{152}H_{258}N_8$	83.2 (83.1)	11.8 (11.8)	4.9 (5.1)	66.2(K→D_3;67); 84.(D_3→D_1;1.1); 94.0(D_1→I; 61)	[e]0.88 (t, 24 H), 1.25 (m, 160 H), 1.5 (m, 16 H), 1.92 (m, 16 H), 2.38 (m, 16 H), 4.75 (t, 16 H), 7.9 (s, 8 H); [730 (1.18), 700 (1.03), 670 (0.38), 635 (0.28)]; {355 (0.53), 310 (0.43)}
6d, 14% $C_{176}H_{306}N_8$	83.3 (83.4)	12.0 (12.2)	4.2 (4.4)	79.3(K→D_1;160); 98.2(D_1→I; 130)	[f]0.92 (t, 24 H), 1.2-1.4 (m, 224 H), 1.6 (m, 16 H), 2.05 (m, 16 H), 4.45 (t, 16 H), 7.85 (s, 8 H); [730 (1.26), 700 (1.08), 665 (0.39), 635 (0.28)]; {360 (0.54), 310 (0.42)}
7a, 85% $C_{112}H_{176}N_8Zn$	78.8 (79.1)	10.1 (10.4)	6.2 (6.6)	89.6(K→D_3; 71); 106.6(D_3→D_1; —); 225.1(D_1→I; 12)	[d]0.92 (t, 24 H), 1.3 (m, 112 H), 1.54 (m, 16 H), 1.8 (m, 16H), 2.41 (m, 16 H), 4.75 (t, 16 H),7.9 (s, 8H); [700 (2.18), 665sh (0.33), 635 (0.38)]; {350 (0.56), 310 (0.43)}
7b, 91% $C_{128}H_{208}N_8Zn$	79.8 (79.9)	10.9 (10.9)	5.6 (5.8)	60.0(K→D_3; 54); 88.5(D_3→D_1;50); 205.6(D_1→I; 7.1)	[d]0.92 (t, 24 H), 1.3 (m, 112 H), 1.55 (m, 16 H), 1.88 (m, 16H), 2.5 (m, 16 H), 4.86 (t, 16 H), 7.96 (s, 8H); [700 (2.07), 665sh (0.32), 635 (0.37)]; {350 (0.50), 310 (0.38)} ms (MALDI): m/z: isotopic cluster at 1924 [M + H]⁺[g]
7c[h], 82% $C_{154}H_{258}N_8ZnCl_6$	74.5 (74.8)	10.5 (10.5)	4.3 (4.5)	65.3(K→D_3; 49); 88.1(D_3→D_2; 35); 103.6(D_2→D_1; 11); 176.2(D_1→I; 2.9)	[d]0.92 (t, 24 H), 1.2 (m, 160 H), 1.42 (m, 16 H), 1.75 (m, 16 H), 2.35 (m, 16 H), 4.7 (t, 16 H), 7.9 (s, 8 H); [700 (1.87), 670sh (0.31), 635 (0.33)]; {350 (0.46), 310 (0.34)} ms (MALDI): m/z: isotopic cluster at 2260 [M + H]⁺[g]
7d[h], 41% $C_{177}H_{305}N_8ZnCl_3$	78.8 (78.4)	11.4 (11.3)	4.0 (4.1)	65.9 (K→D_3; 70); 91.0(D_3→D_2; 18); 108.1(D_2→D_1; 67); 160.5(D_1→I; 1.5)	[f]0.92 (t, 16 H), 1.1-1.7 (m, 240 H), 2.18 (m, 16 H), 4.55 (t, 16 H), 7.85 (t, 8 H); [700 (2.07), 670sh (0.35), 635 (0.37)]; {355 (0.51), 310 (0.39)} ms (MALDI): m/z: isotopic cluster at 2597 [M + H]⁺[g]

[a]Mp or transition temperature for change from the crystalline state to a discotic mesophase (K→D_1), from one mesophase to another (D_i→D_{i+1}) or from a mesophase to an isotropic liquid (D_i→I), i=1, 2 or 3. The number that follows each indicated transition represents the enthalpy for that phase change as measured by DSC in kJ mol⁻¹. Where no value is given, ΔH was too small to measure. For **6b**, the transition D_1→I at 115.5°C actually represents the combined energy for two phase changes due to the fact that two partially overlapping peaks could not be resolved. Energy data for K→D_i transitions were from cooling cycles (rate 5°C min⁻¹), other transition enthalpies were from heating cycles. [b]In C_6D_6. [c]In THF at 25°C. [d]At 25°C. [e]sh=shoulder. [f]In $CDCl_3$ at 40°C. [g]MALDI-TOF ms data. An isotopic cluster peaking at the indicated m/z value for [M + H]. [h]Elemental analysis calculated for **7c**·2CHCl₃ or **7d**·CHCl₃. These solvent molecules, or impurities, may imply that transition temperatures, spectroscopic and CV data for these two compounds may not be precise.
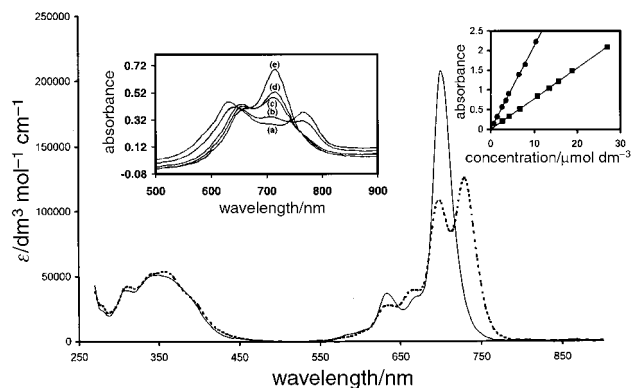
Fig. 1 UV/VIS solution (THF) spectra at 25 °C of **6d** (---) and **7d** (—) showing the Q and Soret bands at *ca.* 700–730 and 350–360 nm respectively. Left insert: The Q-band of a *ca.* 1000 Å thick film of **7b** on glass at 30 ((a), crystalline solid phase K), 80 ((b), mesophase D$_3$), 130 ((c), mesophase D$_1$), 180 ((d), also mesophase D$_1$) and 230 °C ((e), isotropic liquid I). Right insert: The Beer–Lambert law, $A = \varepsilon cl$, [shown at 700 nm for **7a** (●) and 730 nm for **6a** (■)] is valid for all compounds **6** and **7**, indicating aggregation is not a factor in the investigated concentration ranges.

corresponding lithium phthalocyanines was more efficient over 18 hours than over shorter (∼5 h) reaction times. The lithiated phthalocyanines were converted into the metal-free derivatives, **6**, by acid work-up. The complexation of Zn^{2+} with series **6** to give **7** were very efficient reactions, with yields >90% over 2 hours. It was notable that attempts to obtain zinc phthalocyanines directly by reacting **5** (R = C$_{10}$H$_{21}$) with ZnBr$_2$ in the presence of dimethylaminoethanol (DMAE) according to the procedure of Torres and co-workers,[21] failed. Only the metal free phthalocyanine was obtained following work-up with acetic acid. Purification of the phthalocyanines **6** and **7** became more difficult with increased chain lengths. They suffered co-precipitation of impurities or incorporation of solvent molecules upon crystallisation. In addition, the C$_{18}$ substituted phthalocyanines **6** and **7** were only marginally soluble in THF but insoluble in all other common organic solvents at room temperature. They do, however, dissolve well in warm chloroform or THF. Even after rigorous purification procedures, the elemental analysis of the ZnPc–C$_{15}$ and ZnPc–C$_{18}$ derivatives were still marginal. Apart from explaining this by solvent co-precipitation (see Table 2), it should be noted that many phthalocyanines are notoriously difficult to combust.[22] However, these two compounds are deemed to be pure by chromatography, spectroscopy and matrix-assisted laser de-
sorption/ionisation time-of-flight mass spectrophotometry (MALDI-TOF ms). ^{1}H NMR data for all synthesised compounds confirmed their purity and structure and

followed the same trends as described before[23] for the lower homologues; data are summarised in Tables 1 and 2. The solubility properties of the C$_{18}$ compound prepared in this study stand in contrast to what was found for the C$_4$–C$_{10}$ range of octa-alkylated phthalocyanines. It was previously documented that the solubility of octa-alkylated phthalocyanines in the C$_4$–C$_{10}$ alkyl chain length range generally increased.[12] This result is in accordance with the rule of thumb that the solubility of phthalocyanines is enhanced by bulky substituents.[24] Our results with the C$_{18}$ derivative, therefore, indicate that there is a limit to which the solubility of phthalocyanines can be enhanced by simply increasing the size of the substituent.

UV/VIS spectroscopy

All metal-free phthalocyanines are turquoise green while the zinc derivatives are bright blue in the crystalline state. In solution, however, both the metal-free and zinc compounds appear to have a turquoise green colour. The characteristic UV (Soret band) and intense visible region (Q-band) absorptions of the phthalocyanines are documented in Table 2. Metal-free and metal-containing phthalocyanines differ in having D_{2h} and D_{4h} symmetry respectively and this is manifested in differences especially in the Q-band region. The metallated phthalocyanines all showed a single intense maximum at about 700 nm. However, degeneracy of the lowest energy singlet state of the metallated derivatives is lifted in the metal-free derivatives. This leads to a splitting of the Q-band into a Q$_x$ and Q$_y$ component at about 729 and 698 nm (Fig. 1). The low intensity bands at shorter wavelengths than the Q-band, *ca.* 665 and 630 nm, are vibronic in origin. It is known that aggregation of phthalocyanines in solution significantly lowers the extinction coefficients of solutions of these compounds.[12,16] The extinction coefficients, ε, reported in Table 2 were obtained from measurements on solutions in the concentration range 1–25 μmol dm^{-3} for series **6** and 1–10 μmol dm^{-3} for series **7**. No variation of ε was detected which implied phthalocyanine aggregation is absent in this concentration range (Fig. 1).

Mesophase behaviour

The phase transformations from crystalline solid to discotic mesophase (K→D$_i$) and from discotic mesophase to isotropic liquid (D$_i$→I), $i = 1$, 2 or 3, were investigated using polarised optical microscopy. In many cases the colour and/or texture
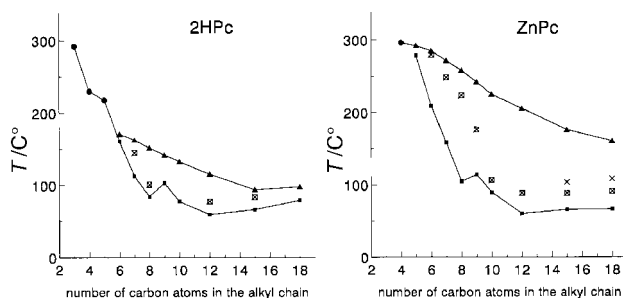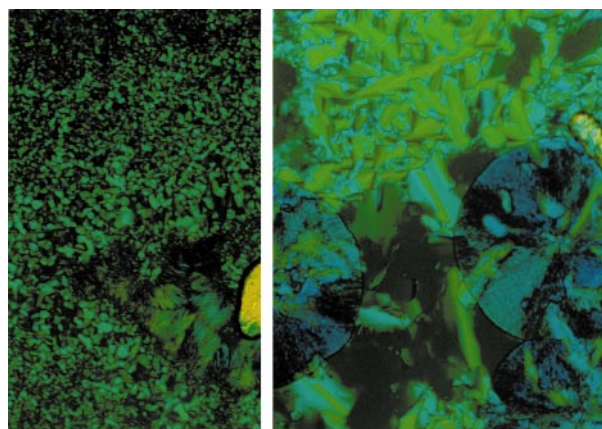

Fig. 2 The temperature range in which the zinc phthalocyanines, ZnPc, right, are liquid crystalline is much larger than for the metal-free derivatives, 2HPc, left. The temperatures at which the transitions took place were determined on a polarised optical microscope. ΔH for each phase change as well as limitations to the data for the ZnPc–C$_{15}$ and ZnPc–C$_{18}$ derivatives are as per Table 2.

Fig. 3 Left: Photograph showing simultaneously the fan (D$_1$, majority of graph) and needle (D$_2$, next to the yellow spot, needles are bundled together in the form of fibres) texture of **6c**. The mixed texture was obtained by cooling **6c** at 10 °C min^{-1} from 95 to 90 °C and then slowly heating (2 °C min^{-1}) to 92 °C. Right: Photograph showing simultaneously the blue crystalline phase (K) and green D$_2$ mesophase with a mosaic pattern. The mixed texture was obtained by cooling **6c** at a rate of 5 °C min^{-1} and the photograph was taken at 66–67 °C.

changes from one mesophase to another were extremely subtle and thus difficult to detect with an optical microscope. The results reported in Table 2 and Fig. 2, therefore, represent the combined conclusions obtained from differential scanning calorimetry (DSC) as well. However, a detailed discussion on the DSC results, together with those from an electrochemical investigation of a series of different metallated phthalocyanines, will be given in a subsequent paper.[25] At least two mesophases denoted as D_1 and D_2, where D_1 is the highest temperature mesophase, were detected for all compounds except the C_{10} and C_{18} metal-free phthalocyanines. The absence of an observable second mesophase for the C_{10} and C_{18} metal-free derivative does not preclude its existence, but it was not observable by the measuring methods at our disposable. The C_{15} and C_{18} zinc phthalocyanines are the first examples of the series 7 class of phthalocyanines to show three observable mesophases, D_1, D_2 and D_3, between the crystalline and isotropic liquid states. The only other compound within the series of complexes thus far studied (Zn, Cu, Ni, Co and 2H complexes having substituents with C_4–C_{10} chainlengths)[11] that showed three observable mesophases (discotic and monotropic), was the 2HPc–C_8 species. In previous reports on the C_4 to C_{10} derivatives,[11] different mesophases were tentatively assigned by comparing the optical textures observed under the polarising microscope with those whose packing symmetries were previously determined from X-ray diffraction studies. These designations were D_{hd}, a discotic disordered mesophase phase showing a fan like texture and comprised of columns of cofacially stacked molecules arranged within a two dimensional hexagonal lattice symmetry, a second disordered hexagonal mesophase, D_{hd}, with a needle-like texture and a third disordered mesophase possessing rectangular symmetry, D_{rd}, which is characterised by a mosaic texture. In the cases reported hitherto, the fan texture of the D_{hd} mesophase was observed at the first transition upon cooling from the isotropic liquid. The needle texture was infrequently observed upon further cooling and the mosaic texture was associated with the mesophase just prior to conversion to a solid crystal. In these previous reports, texture appearances could be generated reversibly and unambiguously. In this study, we found that the texture observed under the microscope was very much a function of the rate of cooling or heating. In the case of the C_{15} metal-free derivative it was found that a fast cooling rate (10 °C min⁻¹) resulted in a needle-like texture upon cooling from the isotropic liquid at 94 °C (I→D_1transition). A slow cooling rate (2 °C min⁻¹) resulted in a texture which resembled, but was not clearly, the fan for the same transition. However on heating the needle-like texture from 90 to 92 °C, it slowly converted in appearance from the needle texture to the fan-like texture. No colour change was observed for this texture change. The photograph in Fig. 3 (left) shows both the needle-like bundles stacked together to create the appearance of fibres and the 'fan-like' texture observed during this transition. Further cooling produces a clear colour change from greenish to bluish when crystallisation (D→K transformation) sets in. In many heating and cooling cycles subtle changes from an apparent 'mosaic' to a fan-like texture was also observed as shown in Fig. 3 (right). It appears that although the long-chain alkylated phthalocyanines of the present study do follow the same general trends as described before,[11] the amount of disorder within the cofacially arranged two dimensional molecular columns are much more pronounced than was experienced with the shorter chain derivatives.

Accordingly, although by analogy to previous studies the observed phases D_1, D_2 and D_3 are expected to conform to the D_{rd}, fan; D_{hd}, needle, and D_{hd}, mosaic, two dimensional symmetry or packing modes, in the absence of X-ray diffraction studies, no definite assignment to this effect can be made. A possible explanation for the less than distinct

mesophase transitions observed in the present study may arise from the length of the side chains of the title compounds. It is quite conceivable that the long chain length of the substituents on phthalocyanines 6 and 7 interfere with the ease by which any semi-ordered liquid crystalline packing may be achieved. This interference will result in a slower formation of any order in the packing of the liquid crystalline phase and it may lead to pronounced distortions in molecular packing.

As can be seen in Fig. 2, the zinc derivatives showed liquid crystalline behaviour over a much larger temperature range than the metal-free derivatives, indicating that zinc has the capability of stabilising mesophases at higher temperatures compared to hydrogen. The C_{12} macrocycle proved to be a turning point. It showed the lowest K→D transition temperature (60.0 °C) of all phthalocyanines investigated thus far in this series and it showed mesophase behaviour over a 145.6 °C temperature range. Only the C_8 derivative had a larger mesophase behaviour temperature range (153.2 °C). The minimum K→D transition temperature of 60 °C indicates that C_{12} alkyl chains approach the limiting length where the waxy (amorphous) properties of long chain alkyl substituents do not substantially override the liquid crystalline properties of the molecule as a whole. The slow increase in K→D transition temperatures at higher chain lengths is typical of the increase in melting points for waxes with an increase in chain length as illustrated by the melting points of tetrakis(decyl)ammonium bromide (89 °C) and tetrakis(octadecyl)ammonium bromide (103 °C).

The insert in Fig. 1 shows the Q-band absorbtion of the ZnPc–C_{12} compound, 7b, cast as a thin film on glass at a temperature within each of the crystalline, discotic mesophases and isotropic liquid phases. The spectrum at 30 °C (i.e. of the compound in crystalline form, the line labelled (a)) shows two peaks at 630 and 765 nm respectively. The spectrum at 80 °C (line (b)) is of the compound in the low temperature mesophase, D_3. The peak at 630 nm was shifted to 642 nm, while the 765 nm peak was not moved. The appearance of a new peak at 714 nm is, however, faintly apparent. At the top end of the second, high-temperature (D_1), mesophase temperature range, at 180 °C, the spectrum (line (d)) shows a distinct new peak at 714 nm while the peak at 765 nm has disappeared. A weaker peak is also observed at 658 nm. A spectrum of the compound at 230 °C (i.e. in the isotropic liquid state, line (e)) shows an intense Q-band maximum at 714 nm together with a shoulder at 666 nm. The appearance of the spectrum of the isotropic liquid is very similar to that of the compound in solution, which showed Q_{max} at $\lambda = 700$ nm and a shoulder at 665 nm. Thin film variable temperature visible spectra of the C_{15} and C_{18} zinc phthalocyanines had the same features and followed the same trend. The spectrum of spin coated films of the metal free derivatives also showed two peaks (at $\lambda = 640$ and 771 nm at 35 °C for the C_{12} compound) in the crystalline state which collapsed to Q_x and Q_y bands with $\lambda_{max} = 734$ and 704 nm upon heating to a temperature above the transition temperature for isotropic liquid formation. With one exception, all peak maxima for the C_{15} and C_{18} compounds (metal-free and zinc-containing) were within 5 nm of those of the C_{12} derivative. Only the lower wavelength peak of the metal-free C_{18} compound differed in that it was broadened with an additional shoulder at 674 nm.

Cyclic voltammetry

Cyclic voltammetry results, obtained from ca. 1 mM solutions of the compounds in either dichloromethane or 1,2-dichloroethane, are summarised in Table 3. Although the four observed redox signals in the potential range −1.8 to 1.2 V vs. Ag/Ag⁺ were more ideal for the metal free phthalocyanines (2HPc), 6, than for the zinc derivatives, ZnPc, neither exhibited ideal reversible behaviour. Electrochemical reversibility for one-electron processes at 25 °C is characterised by peak potential

Table 3 Peak anodic, E_{pa}, or peak cathodic potentials, E_{pc} (*versus* Ag/Ag⁺); difference between peak anodic and peak cathodic potentials, ΔE_p; formal reduction potentials, $E^{0\prime}$; peak cathodic, i_{pc}, or peak anodic currents, i_{pa}; and peak current ratios, i_{pc}/i_{pa} or i_{pa}/i_{pc}, for the indicated compounds (concentrations 1 mmol dm⁻³) in 1,2-dichloroethane (unless otherwise stated) with 0.1 mol dm⁻³ tetrabutylammonium hexafluorophosphate as supporting electrolyte at the indicated scan rates and temperatures. Ferrocene itself, under identical conditions but in the absence of any phthalocyanines, had ΔE_p, =90 mV at 25 °C and 107 mV at 70 °C, i_{pa}/i_{pc}, 0.97–1.00 at scan speeds, v=50–200 mV s⁻¹, $E^{0\prime}$ = 0.220 V at 25 °C or 0.246 V at 70 °C *vs.* a Ag/Ag⁺ reference electrode in dichloromethane or 1,2-dichloroethane

	Wave I					Wave II					Wave III					Wave IV				
v/mV s⁻¹	E_{pc}/V	ΔE_p/mV	$E^{0\prime}$/V	i_{pc}/μA	i_{pc}/i_{pa}	E_{pc}/V	ΔE_p/mV	$E^{0\prime}$/V	i_{pc}/μA	i_{pc}/i_{pa}	E_{pa}/V	ΔE_p/mV	$E^{0\prime}$/V	i_{pa}/μA	i_{pa}/i_{pc}	E_{pa}/V	ΔE_p/mV	$E^{0\prime}$/V	i_{pa}/μA	i_{pa}/i_{pc}
1,4,8,11,15,18,22,25-octadecylphthalocyanine (2HPc-C₁₀, 6a, at 25 °C in dichloromethane)																				
50	−1.635	142	−1.564	2.38	1.54	−1.230	96	−1.181	2.38	1.39	0.403	88	0.359	2.77	0.98	0.779	93	0.733	2.04	∞
100	−1.665	180	−1.575	3.27	1.90	−1.235	120	−1.175	3.57	1.92	0.403	88	0.359	3.80	1.03	0.805	146	0.732	2.38	15
150	−1.689	203	−1.588	3.72	1.95	−1.240	132	−1.175	4.62	2.17	0.403	88	0.359	4.62	1.05	0.851	219	0.742	2.71	11
200	−1.689	212	−1.583	4.02	2.01	−1.243	144	−1.171	5.36	2.26	0.403	88	0.359	5.37	1.06	0.862	235	0.745	3.05	9
1,4,8,11,15,18,22,25-octa-alkylphthalocyanines (2HPc's, v=50 mV s⁻¹, 6b at 25 °C, 6c and 6d at 75 °C)																				
6b[a]	−1.619	156	−1.541	1.33	1.99	−1.265	154	−1.188	1.27	1.02	0.418	75	0.380	1.32	1.06	0.929	233	0.813	1.30	—[b]
6c[a]	−1.660	194	−1.563	—	—	−1.245	130	−1.180	2.22	1.07	0.450	120	0.390	2.35	1.08	1.057	151	0.982	1.71	—[b]
6d[a]	?[d]	—	—	—	—	−1.338[b]	236[b]	−1.220[b]	1.33[b]	4.43[b]	0.497	168	0.413	1.25	1.06	0.948[b]	104[b]	0.896[b]	0.397[b]	—[b]
zinc 1,4,8,11,15,18,22,25-octadecylphthalocyanine (ZnPc-C₁₀, 7a, T=75 °C)																				
50	−1.680	246	−1.557	—	—	−1.408	146	−1.335	1.80	—[b]	0.271	105	0.219	2.17	1.12	0.944	128	0.880	1.89	2.52
100	−1.700	262	−1.569	—	—	−1.418	156	−1.340	2.26	—[b]	0.270	104	0.218	2.84	1.09	0.947	149	0.873	2.14	2.14
150	−1.721	280	−1.581	—	—	−1.427	165	−1.344	2.53	9.5[b]	0.279	113	0.222	3.32	1.13	0.961	190	0.866	2.37	1.95
200	−1.742	300	−1.592	—	—	−1.443	181	−1.352	2.72	35[b]	0.285	123	0.223	3.63	1.14	0.990	230	0.875	2.51	1.86
zinc 1,4,8,11,15,18,22,25-octa-alkylphthalocyanines (ZnPc's, 7b–d, v=50 mV s⁻¹, T=75 °C)																				
7b[a]	?[c]	—	—	—	—	−1.404[b]	148[b]	−1.330[b]	0.98[b]	—[b]	0.342	129	0.277	1.53	1.04	0.976	164	0.894	1.61	2.72
7c[a]	?[c]	—	—	—	—	−1.500[b]	121[b]	−1.439[b]	0.24[b]	—[b]	0.360	138	0.294	0.81	0.95	0.996[b]	211[b]	0.891	—[b]	—[b]
7d[a]	?[c]	—	—	—	—	—	—	?[c]	—	—	0.365	147	0.292	0.26	1.09	0.950[b]	—	—	—	—

[a] Compound number. [b] Poorly defined wave. Where possible an estimated value is given. [c] No clear-cut peak observed, no estimates possible. [d] $E_{pa} \approx$ −1.437 V. Restrictions to the accuracy of data referring to **7c** and **7d** are as per Table 2.
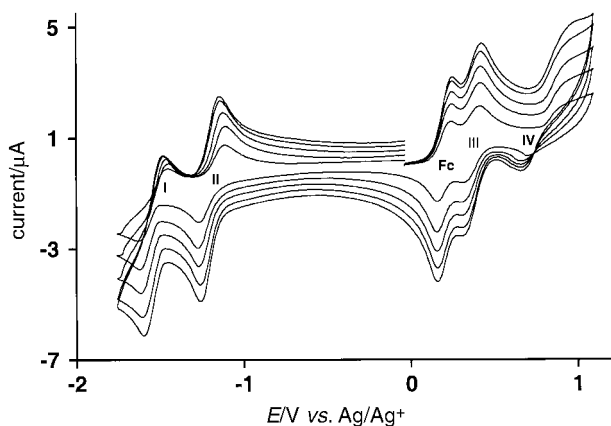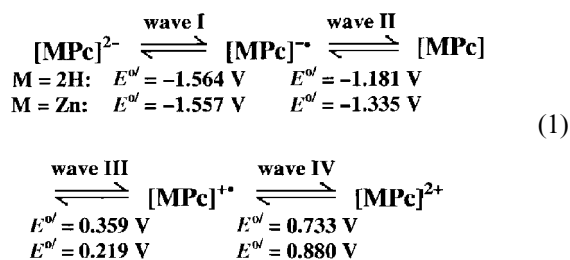
Fig. 4 Cyclic voltammograms showing the four ring centred redox processes I, II, III and IV of **6b** in 1,2-dichloroethane (1 mmol dm^{-3}) containing 0.1 mol dm^{-3} tetrabutylammonium hexafluorophosphate at scan rates 50 (smallest i_p values), 100, 150, 200 and 250 mV s^{-1} on a Pt working electrode at 25 °C. The peak labelled Fc is that of ferrocene that has been added as an internal marker to the solution containing **6b**.
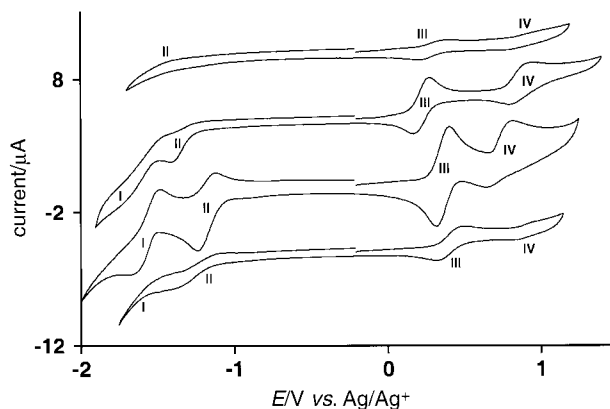

Fig. 5 Cyclic voltammograms of (in order from bottom to top) **6d**, **6a**, **7a** and **7d**, showing the four ring centred redox processes I, II, III and IV in 1,2-dichloroethane (1 mmol dm^{-3}) containing 0.1 mol dm^{-3} tetrabutylammonium hexafluorophosphate at 70 °C at a scan rate of 50 mV s^{-1} on a Pt working electrode at 75 °C. Conditions for **6a** only: in dichloromethane at 25 °C. Limitations to the data for the ZnPc–C$_{18}$ derivative are as per Table 2.

differences of 59 mV and is independent of scan rate.[26] The 2HPc–C$_{10}$ and 2HPc–C$_{12}$ derivatives showed good, well defined, CV's in dichloromethane or 1,2-dichloroethane at 25 °C (Fig. 4). For all the other compounds, peak currents tended to approach zero at room temperature and better results were obtained at 70 °C in 1,2-dichloroethane. However, even at 70 °C in 1,2-dichloroethane, only one well identified quasi-reversible peak at 0.292 mV was observed (Fig. 5) for the ZnPc–C$_{18}$ derivative.

All four observed redox processes are associated with the ring-based electron transfer couples [MPc]$^{2-}$/[MPc]$^{-\bullet}$ (wave I, Fig. 4 and 5), [MPc]$^{-\bullet}$/[MPc] (wave II), [MPc]/[MPc]$^{+\bullet}$ (wave III) and [MPc]$^{+\bullet}$/[MPc]$^{2+}$ (wave IV) with M = 2H or Zn as demonstrated in eqn. (1). Regarding 2HPc's, except for wave IV, the chain length of the substituted alkyl groups did not result in changes in the formal reduction potentials, $E^{o\prime} = (E_{pa}+E_{pc})/2$ where E_{pa} and E_{pc} are the peak anodic and peak cathodic potentials respectively, of more than 30 mV (Table 3). However, the 2HPc–C$_{18}$ derivative showed anomalous behaviour in that wave I could not be observed and wave IV was poorly defined under our experimental conditions. Also, $E^{o\prime}$ of wave III was 50 mV more positive than that of the C$_{10}$ compound. $E^{o\prime}$ for wave IV became 80 and 160 mV more positive when moving from the 2HPc-C$_{10}$ to the C$_{12}$ and C$_{15}$ compounds respectively. $E^{o\prime}$ values, at a scan rate of 50 mV s^{-1} vs. Ag/Ag$^+$, shown in eqn. (1), refer to the C$_{10}$ compound.

$$\text{[MPc]}^{2-} \xrightleftharpoons[\text{wave I}]{} \text{[MPc]}^{-\bullet} \xrightleftharpoons[\text{wave II}]{} \text{[MPc]}$$

M = 2H: $E^{o\prime} = -1.564$ V $E^{o\prime} = -1.181$ V
M = Zn: $E^{o\prime} = -1.557$ V $E^{o\prime} = -1.335$ V

$$\xrightleftharpoons[\text{wave III}]{} \text{[MPc]}^{+\bullet} \xrightleftharpoons[\text{wave IV}]{} \text{[MPc]}^{2+}$$

$E^{o\prime} = 0.359$ V $E^{o\prime} = 0.733$ V
$E^{o\prime} = 0.219$ V $E^{o\prime} = 0.880$ V

(1)

Poor solubility of unsubstituted phthalocyanines precludes solution phase electrochemistry of these compounds in non-coordinating solvents such as CH$_2$Cl$_2$ or 1,2-dichloroethane. To overcome this, Campbell[27] studied the unsubstituted metal-free phthalocyanine at 150 °C in 1-methylnaphthalene. Only two reduction waves at −0.92 and −1.37 V versus Ag/Ag$^+$ were reported. However, five formal reduction potentials at 0.33, −0.97, −1.37, −2.24 and −2.51 V versus a Ag/Ag$^+$ reference electrode are on record[28] for the unsubstituted 2HPc species in DMF. Literature cited potentials were originally

reported versus SCE but in this work, to allow direct comparison with our results, were adjusted to be versus a Ag/Ag$^+$ (from 0.1 mol dm^{-3} AgNO$_3$ in acetonitrile) reference electrode, which has a potential of +0.31 V versus SCE as reported elsewhere.[29] Our octa-substituted metal free complexes showed one more oxidation process at 0.733 V but the two more negative reduction processes could not be detected under our experimental conditions.

Compared to the unsubstituted phthalocyanine, the effect of octa-alkyl substitution makes the first oxidation process (wave III) ca. 0.03 V more positive, and both the first (wave II) and second (wave I) reduction processes about 0.20 V more negative. Likewise, in DMF, formal reduction potentials for the one observed oxidation and four observed reduction waves for unsubstituted zinc phthalocyanines[28,30] are 0.36, −1.17, −1.61, −2.16 and −2.56 V versus Ag/Ag$^+$ respectively. At 150 °C in non-coordinating 1-methylnaphthalene one oxidation wave at 0.45 and two reduction processes at −1.09 and −1.45 V are reported.[27] Under our experimental conditions (70 °C, 1,2-dichloroethane), the octa-alkylated ZnPc's showed a second oxidation peak, but the two most negative reduction processes reported for ZnPc itself could not be detected. As can be seen from eqn. (1), the first oxidation wave for our complexes was observed at 0.219 V, some 0.14 V less positive than for the unsubstituted compound in DMF, while the first reduction wave was observed at ca. −1.335 mV, ca. 0.17 V more negative in character. Surprisingly, the second reduction wave of our compounds coincided almost exactly with that of unsubstituted ZnPc in DMF at −1.557 V versus Ag/Ag$^+$.

The two reduction waves, waves I and II (eqn. (1)) were very poorly defined for all our Zn complexes and became worse as the chain length of the alkyl substituents increased. For the ZnPc–C$_{18}$ derivative, the only readily identifiable peak was that of wave III. When compared to the ferrocene/ferricenium (Fc/Fc$^+$) couple, wave III for the 2HPc–C$_{10}$ and 2HPc–C$_{12}$ compounds were essentially reversible in either dichloromethane or 1,2-dichloroethane. When free ferrocene is used as an internal marker in the presence of 2HPc's (Fig. 4) according to the method described by Gagne,[31] a slightly better ΔE_p value of 83 mV for the ferrocene signals is observed, but $E^{o\prime}$ for the Fc/Fc$^+$ couple shifted to 201 mV vs. Ag/Ag$^+$ compared to 220 mV (Table 3) in the absence of any phthalocyanines. The drift in $E^{o\prime}$ for ferrocene in the presence of phthalocyanines is probably a consequence of the closeness of $E^{o\prime}$ of wave III, see eqn. (1) above and Fig. 4, to that of the Fc/Fc$^+$ couple. For the Zn derivatives, these two potentials are

overlapping so much that peak separation was not possible. For this reason we chose to give our experimentally determined potentials *versus* Ag/Ag$^+$ as reference electrode. For the 2HPc–C$_{15}$ compound, ΔE_p values for wave III were 120 mV or larger depending on the scan rate; for the 2HPc–C$_{18}$ derivative ΔE values were 168 mV or larger. The increase in ΔE_p values with increase in alkyl chain length (and also scan rate) indicates that the rate of electron transfer between the electrode and the phthalocyanines are severely hampered by the alkyl side chains and it becomes progressively worse as the side chain length increases. This must be a function of the availability of a non-hindered, efficient route that will allow fast electron flow between the electrode and the phthalocyanine core and can be explained by the length of the side chains on the phthalocyanines. It can be envisaged that the longer the chain length of the eight alkyl substituents, the more efficiently they will coil and wrap around the phthalocyanine core, thereby partially isolating the active redox centre from the electrode.

The peak cathodic and peak anodic current ratio, i_{pc}/i_{pa}, for wave III (2HPc's), approached unity which indicated this electrochemical process was not accompanied by any other physical or chemical process. All the other 2H- and ZnPc's waves investigated here deviated substantially from unity. However, since no additional wave apart from the four belonging to the phthalocyanine system could be detected, we conclude that the deviation from unity in waves I, II and IV is probably not the consequence of a chemical process that accompanies these processes either. Rather, we are of the opinion that the lack of suitable solubility of these *in situ* generated [MPc]$^{2-}$, [MPc]$^{-\bullet}$ and [MPc]$^{2+}$ species in the non-polar solvents dichloromethane or 1,2-dichloroethane disallows the generation of a CV half wave of sufficient intensity during the reverse sweep to maintain i_{pc}/i_{pa} ratios approaching unity. The possibility of these intermediates forming thin coatings by adsorption on the electrode, as described elsewhere,[32] is to a large extent limited in view of the protective layer, or globule, that the eight long alkyl substituents apparently form around the phthalocyanine core. It appears that the consequence of this wrapping of side chains around the phthalocyanine core to effectively encapsulate it, in certain circumstances proves to be beneficial, while in other cases not.

Experimental

Materials

Reagents (Lancaster or Aldrich) were used without further purification. Dry, air-free THF was obtained by refluxing under nitrogen over sodium metal and distillation just prior to use. Water was purified through a standard Millipore system to a resistivity of at least 18 MΩ cm. Fluka silica gel 60 grade 60741 was used in chromatographic separations. TLC was performed using Fluka grade 60778 silica gel on aluminium sheets.

Thin film preparation

Cleaning of glass slides for thin film deposition: Microscope glass slides (BDH) were wiped with Kimwipe paper, washed in a stream of methanol and then sonicated for 5 minutes in water containing 2–4% Decon 24 (Fisher), cleaned with a stream of water, sonicated in pure water, and dried in a stream of propan-2-ol.

Films: Spin-coated films of all phthalocyanines were prepared at room temperature (50 °C for the C$_{18}$ derivatives) from THF solutions (2.5 mg in 0.1 ml) dropped on a previously cleaned microscope glass slide rotating at 2000 rpm using a spinner (Headway Research, Inc.). Spinning was continued for 20 s by which time the solvent had evaporated. Previous measurements of film thickness (mechanical stylus equipment)

have established that films formed under these conditions are *ca.* 1000 Å thick.[33]

Spectroscopy

Proton NMR-spectra at 298 K were recorded at 270 MHz on a JEOL EX 270 instrument and chemical shifts are referenced to SiMe$_4$ at 0.00 ppm. IR spectra (thin films between NaCl plates of either pure liquids or Nujol mulls of solids) were recorded on a Perkin Elmer 297 instrument. Conventional electronic spectra were recorded in THF on a Varian Cary 50 UV/VIS dual beam spectrophotometer at 25 °C. Thin film variable temperature visible spectra were recorded on a Hitachi U-3000 spectrophotometer fitted with a near-infrared sensitive detector and polaroid polarizers. The film-bearing substrate was located in a Mettler FP82 hotstage, orientated orthogonally to the incident beam and controlled by an FP80 Processor. MALDI-TOF mass spectra were obtained using a Kratos Kompact MALDI 3 with a dithranol matrix at the University of Manchester.

Differential scanning calorimetry and microscopy

Transitions between crystal, liquid crystal and isotropic liquid states were monitored by DSC (for enthalpy changes, *ca.* 7 mg samples at heating and cooling rates of 10 °C min^{-1} between −70 °C and a convenient maximum temperature at least 30 °C higher than the melting point of the compounds) using a TA Instruments DSC 10 thermal analyser fitted with a DuPont Instruments mechanical cooling accessory and a TA Instruments Thermal Analyst 2000 data processing unit. Visual measurements (to obtain transition temperatures) were performed on an Olympus BH-2 polarising microscope in conjunction with a Linkam TMS 92 thermal analyser with a Linkam THM 600 cell. The heating and cooling rates used were either 5 °C min^{-1} or 2 °C min^{-1}.

Cyclic voltammetry

Measurements utilizing *ca.* 1 mmol dm^{-3} phthalocyanine solutions at 25 °C in dichloromethane, for 2H–C$_{10}$ and 2H–C$_{12}$ derivatives, or at 70 °C in 1,2-dichloroethane for all compounds except the 2H–C$_{10}$ derivative, with 0.100 mol dm^{-3} tetra-*n*-butylammonium hexafluorophosphate (Fluka, electrochemical grade) as supporting electrolyte, were conducted under a blanket of purified argon utilising a BAS model CV-27 voltammograph interfaced with a personal computer. A three-electrode cell, which utilized a Pt-auxiliary electrode, a Pt working electrode with surface area 0.0707 cm^2, and a Ag/Ag$^+$ (0.100 mol dm^{-3}, AgNO$_3$ in acetonitrile) reference electrode[34] mounted on a Luggin capillary[35] filled with a 0.100 mol dm^{-3} supporting electrolyte solution in acetonitrile, was employed. Data, uncorrected for junction potentials, were collected with an Adalab-PC^{TM} and Adapt^{TM} data acquisition kit (Interactive Microwave, Inc.) with locally developed software, and analysed with Hyperplot (JHM International, Inc.). All temperatures were kept constant to within 0.2 °C.

Synthesis

Only one representative example is provided for each of the general methods.

2,5-Dialkylthiophenes   3. *2,5-Bis(octadecyl)thiophene (Table 1, 3d).* To a stirred solution of thiophene (8.4g, 0.1 mol) in THF (dried over sodium; 50 cm^3), precooled to −75 °C in a CO$_2$(s)–acetone bath, was added under nitrogen over 30 min *n*-butyllithium in hexane (100 cm^3 of a 2.5 mol dm^{-3} solution, 0.25 mol, 2.5 equivalents). After the addition was completed the reaction mixture was allowed to spontaneously heat up to room temperature, while stirring

continued for 24 h at room temperature. The dilithiated species **2a** that formed during this time was not isolated but treated *in situ* at −75 °C under nitrogen over 30 min with 1-bromoocta-decane (83.35 g, 0.25 mol). The stirred reaction mixture was then allowed to warm to room temperature. After 24 hours it was poured onto ice, the product extracted with diethyl ether (3×75 cm^3) and the organic extracts dried (MgSO$_4$) and filtered. Removal of solvents followed by recrystallisation of the residue from diethyl ether or warm ethanol gave *2,5-bis(octadecyl)thiophene* **3d** (55.4 g, 94%) as an off-white solid, mp 56 °C (Found: C, 81.6; H, 13.0; S, 5.5. C$_{40}$H$_{76}$S requires C, 81.6; H, 13.0; S, 5.4%); δ_H(270 MHz, CDCl$_3$) 0.88 (6 H, t, $2 \times$ CH$_3$), 1.3 (60 H, m, $30 \times$ CH$_2$), 1.64 (4 H, m, $2 \times$ CH$_2$), 2.71 (4 H, t, $2 \times$ CH$_2$) and 6.48 (2 H, s, C$_4$H$_2$S). Note: The decyl and dodecyl derivatives **3a** and **3b** were fractionally distilled at 0.1 mmHg for purification.

2,5-Dialkylthiophene 1,1-dioxides 4. *2,5-Bis(dodecyl)thiophene 1,1-dioxide (Table 1, 4b), sodium perborate method.* To a stirred mixture of 2,5-bis(dodecyl)thiophene (11.776 g, 20 mmol) in glacial acetic acid (85 cm^3) was added solid NaBO$_3$·4H$_2$O (23.079 g, 150 mmol) over *ca.* 5 min with care being taken to maintain the internal temperature between 48 and 52 °C. The reaction mixture was then stirred at 50 °C for another 5 h before it was left at room temperature for 16 h. The acetic acid was removed under reduced pressure and the solid residue stirred with 80 cm^3 H$_2$O and filtered. The remaining solid was extracted with diethyl ether (100 cm^3) and the organic solution washed with H$_2$O (100 cm^3) and brine (100 cm^3) before it was dried (MgSO$_4$). Removal of the solvent and recrystallisation of the waxy residue from hexane gave *2,5-bis(dodecyl)thiophene 1,1-dioxide* **4b** (1.55g, 17%) as a white solid, mp 73 °C (Found: C, 73.8; H, 11.5; S, 6.8. C$_{28}$H$_{52}$SO$_2$ requires C, 74.2; H, 11.6; S, 7.1%); δ_H(270 MHz, CDCl$_3$) 0.90 (6 H, t, $2 \times$ CH$_3$), 1.3 (36 H, m, $18 \times$ CH$_2$), 1.64 (4 H, m, $2 \times$ CH$_2$), 2.49 (4 H, t, $2 \times$ CH$_2$) and 6.25 (2 H, s, C$_4$H$_2$SO$_2$). Note: This method was not successful for the syntheses of the pentadecyl and octadecyl derivatives **4c** and **4d** respectively.

2,5-Bis(pentadecyl)thiophene 1,1-dioxide (Table 1, 4c), m-chloroperoxybenzoic acid method. A solution of 2,5-bis(pentadecyl)thiophene (10.08 g, 20 mmol) in 250 cm^3 dichloro-methane was stirred with 50–60% *m*-chloroperoxybenzoic acid (12.5 g, ~30 mmol) at 0 °C in the presence of an excess of NaHCO$_3$ (50 g, 77 mmol). The heterogeneous mixture was left standing for 16 hours at 5 °C before all solids were filtered and washed with dichloromethane (2×100 cm^3). The combined organic phases were washed with 20% NaOH (2×100 cm^3), H$_2$O (2×100 cm^3) and dried (MgSO$_4$) to give, after solvent removal and recrystallisation of the waxy residue from warm ethanol, 2,5-bis(pentadecyl)thiophene 1,1-dioxide **4c** (2.0 g, 19%) as a white solid, mp 79 °C (Found: C, 75.9; H, 12.0; S, 6.0. C$_{34}$H$_{64}$SO$_2$ requires C, 76.0; H, 12.0; S, 6.0%); δ_H(270 MHz, CDCl$_3$) 0.90 (6 H, t, $2 \times$ CH$_3$), 1.3 (48 H, m, $24 \times$ CH$_2$), 1.62 (4 H, m, $2 \times$ CH$_2$), 2.48 (4 H, t, $2 \times$ CH$_2$) and 6.25 (2 H, s, C$_4$H$_2$SO$_2$). Note: This method gave C$_{12}$ and shorter chain dialkylated thiophene 1,1-dioxides in 41% yield or better.

2,5-Bis(octadecyl)thiophene 1,1-dioxide (Table 1, 4d), dimethyldioxirane method. To a 2 l 2-neck flask, equipped with an *efficient* stirrer, a large CO$_2$–acetone condenser and charged with H$_2$O (440 cm^3), acetone (320 cm^3) and NaHCO$_3$ (240 g) was added a solution of 2,5-bis(octadecyl)thiophene (11.76 g, 20 mmol) in dichloromethane (360 cm^3). The resulting heterogeneous mixture was cooled in an ice bath before solid oxone (400 g) was carefully added over 30 min under efficient stirring. Stirring continued at room temperature for 16 hours before water (2 l) was added to dissolve most inorganics. The decanted aqueous layer, and all remaining solids were extracted with dichloromethane (1 l), the combined organic phases washed with water (1–2 l) and dried (MgSO$_4$) before solvent

removal and recrystallisation of the residue from ethanol gave pure off-white *2,5-bis(octadecyl)thiophene 1,1-dioxide* **4d** (11.6 g, 94%), mp 88 °C (Found: C, 77.4; H, 12.4; S, 4.7. C$_{40}$H$_{76}$SO$_2$ requires C, 77.4; H, 12.3; S, 5.1%); δ_H(270 MHz, CDCl$_3$) 0.90 (6 H, t, $2 \times$ CH$_3$), 1.28 (60 H, m, $30 \times$ CH$_2$), 1.62 (4 H, m, $2 \times$ CH$_2$), 2.47 (4 H, t, $2 \times$ CH$_2$) and 6.23 (2 H, s, C$_4$H$_2$SO$_2$). Note: this method gave all long chain dialkylated thiophene 1,1-dioxides in high yield.

3,6-Dialkylphthalonitriles 5. *3,6-Bis(octadecyl)phthalonitrile (Table 1, 5d).* In a typical experiment 2,5-bis(octadecyl)thio-phene 1,1-dioxide **4d** (5 g, 8.06 mmol) and fumaronitrile (0.629 g, 8.06 mmol) were introduced into a glass tube using a minimum volume of chloroform (*ca.* 1.5 cm^3). The tube was sealed and heated at 160 °C for 18 h. The contents of the tube were dissolved in chloroform and the solvent evaporated under reduced pressure at 90 °C. The oily residue was kept under reduced pressure until it no longer liberated gas (presumed to be SO$_2$) any more (*ca.* 20–30 min). The remaining residue was chromatographed over silica with toluene as eluent. The second eluted band afforded after solvent removal and recrystallisa-tion from ethanol *3,6-bis(octadecyl)phthalonitrile* **5d** (1.4 g, 27%) as an off-white solid, mp 82 °C (Found: C, 83.6; H, 12.0; N, 4.2. C$_{44}$H$_{76}$N$_2$ requires C, 83.5; H, 12.1; N, 4.4%); ν_{max}(Nujol) 2 230 cm^{-1} (C≡N); δ_H(270 MHz, CDCl$_3$) 0.89 (6 H, t, $2 \times$ CH$_3$), 1.3 (60 H, m, $30 \times$ CH$_2$), 1.63 (4 H, m, $2 \times$ CH$_2$), 2.83 (4 H, t, $2 \times$ CH$_2$) and 7.47 (2 H, s, C$_6$H$_2$). Note: shorter chain alkylated phthalonitriles[12] were obtained in yields approaching 50%.

Metal-free phthalocyanines 6. *1,4,8,11,15,18,22,25-Octakis (pentadecyl)phthalocyanine (Table 2, 6c).* In a typical synth-esis 3,6-bis(pentadecyl)phthalonitrile **5c** (0.800 mg, 1.46 mmol) was dissolved in warm (80 °C) pentanol (8 cm^3). An excess of clean lithium metal (0.3–0.4 g, 43–58 mmol) was added in small portions and the mixture heated for 16 h at 110 °C. The cooled, deep green coloured suspension was stirred with acetone (50 cm^3), the solution filtered and the solids washed with acetone (50 cm^3) before the combined acetone solutions were concentrated to *ca.* 25 cm^3. Acetic acid (50 cm^3) was added, the heterogeneous mixture stirred for 30 minutes and the pre-cipitate collected to afford after recrystallisation from THF–methanol or CHCl$_3$–methanol *1,4,8,11,15,18,22,25-octakis-(pentadecyl)phthalocyanine* **6c** (170 mg, 21%), phase transi-tions as per Table 2 (Found: C, 82.3; H, 11.2; N, 5.6. C$_{128}$H$_{210}$N$_8$·2CHCl$_3$ requires C, 82.6; H, 11.4; N, 6.0%); δ_H(270 MHz, C$_6$D$_6$) 0.90 (24 H, t, $8 \times$ CH$_3$), 1.25 (112 H, m, $56 \times$ CH$_2$), 1.5 (16 H, m, $8 \times$ CH$_2$), 1.85 (16 H, m, $8 \times$ CH$_2$), 2.38 (16 H, m, $8 \times$ CH$_2$), 4.77 (16 H, m, $8 \times$ CH$_2$) and 7.95 (8 H, s, $4 \times$ C$_6$H$_2$). Note: in some experiments it was beneficial to chromatograph the crude product on silica with petroleum ether : THF (99 : 1) prior to recrystallisation. The C$_{18}$ derivative was not soluble enough to allow chromatography.

Zinc-containing phthalocyanines 7. *1,4,8,11,15,18,22,25-Octakis(octadecyl)phthalocyaninatozinc(II) (Table 2, 7d).* A stirred mixture of metal-free 1,4,8,11,15,18,22,25-octakis(octa-decyl)phthalocyanine (**6d**, 240 mg, 0.099 mmol), zinc acetate dihydrate (90 mg, 0.41 mmol) and pentanol (10 cm^3) was heated at 130 °C for 5 h. Methanol (20 cm^3) was added to the cooled reaction mixture and the precipitate filtered and washed with excess methanol. A filtered, concentrated, warm (60 °C) chloroform solution of the collected blue precipitate was submerged in a water bath at 60 °C (to retard the cooling rate) and allowed to cool slowly to room temperature. The collected blue solid was washed thoroughly with cold THF and then with chloroform to yield 1,4,8,11,15,18,22,25-octakis-(octadecyl)phthalocyaninatozinc(II), **7d**, (105 mg, 41%), phase

transitions as per Table 2 (Found: C, 78.8; H, 11.4; N, 3.9. $C_{176}H_{304}N_8Zn\cdot CHCl_3$ requires C, 78.4; H, 11.3; N, 4.1%); δ_H(270 MHz, CDCl$_3$, 40 °C) 0.92 (24 H, t, 8 × CH$_3$), 1.1–1.7 (240 H, m, 120 × CH$_2$), 2.18 (16 H, m, 8 × CH$_2$), 4.55 (16 H, m, 8 × CH$_2$) and 7.85 (8 H, s, 4 × C$_6$H$_2$).

Acknowledgement

References

1 D. Birkett, *Chem. Ind.*, 2000, 178; R. Ao, L. Kilmmert and D. Haarer, *Adv. Mater.*, 1995, **7**, 495; *Phthalocyanines: Properties and Applications*, eds. C. C. Leznoff and A. B. P. Lever, VCH, New York, 1989, vol. 1; *Phthalocyanines: Properties and Applications*, eds. C. C. Leznoff and A. B. P. Lever, VCH, New York, 1992, vol. 2; *Phthalocyanines: Properties and Applications*, eds. C. C. Leznoff and A. B. P. Lever, VCH, New York, 1993, vol. 3; *Phthalocyanines: Properties and Applications*, eds. C. C. Leznoff and A. B. P. Lever, VCH, New York , 1996, vol. 4.

2 K. Kasuga and M. Tsutsui, *Coord. Chem. Rev.*, 1980, **32**, 67; *Organic coating Technology*, Wiley, New York, 1961, **vol. 2**, pp 896–899; C. R. Martens in *Riegel's Handbook of Industrial Chemistry*, ed. J. A. Kent, Van Nostrand-Reinhold, New York, 1974, ch. 22.

3 J. D. Wright, *Prog. Surf. Sci.*, 1989, **31**, 1; A. W. Snow and W. R. Barger in *Phthalocyanines: Properties and Applications*, eds. C. C. Leznoff and A. B. P. Lever, VCH, New York, 1989, **vol. 1**, p. 341; A. W. Snow, W. R. Barger, M. Klusty, H. Wöhltjen and N. L. Jarvis, *Langmuir*, 1986, **2**, 513.

4 H. Ali and J. E. van Lier, *Chem. Rev.*, 1999, **99**, 2379; L. Milgrom and S. Macrobert, *Chem. Br.*, 1998, 45; R. W. Boyle, C. C. Leznoff and J. E. van Lier, *Br. J. Cancer*, 1993, **67**, 1177.

5 G. de la Torre, P. Vázquez, F. Agulló-López and T. Torres, *J. Mater. Chem.*, 1998, **8**, 1671; A. Grund, A. Kaltbeitzel, A. Mathy, R. Schwarz, C. Bubeck, P. Vernmehren and M. Hanack, *J. Phys. Chem.*, 1992, **96**, 7450.

6 D. Wöhrle, D. Schlettwein, M. Kirschenmann, M. Kaneko and A. Yamada, *J. Macromol. Sci. Chem.*, 1990, **A27**, 1239.

7 H. Eichhorn, *J. Porphyrins Phthalocyanines*, 2000, **4**, 88; D. Wöhrle and D. Meissner, *Adv. Mater.*, 1991, **3**, 129.

8 H. Eckert and Y. Kiesel, *Angew. Chem., Int. Ed. Engl.*, 1981, **20**, 473.

9 T. Buck, D. Wöhrle, G. Schulz-Ekloff and A. Andreef, *J. Mol. Catal.*, 1991, **70**, 259.

10 M. J. Cook, G. Cooke and A. Jafari-Fini, *Chem. Commun.*, 1996, 1925; C. Piechocki, J. Simon, A. Skoulious, D. Guillon and P. J. Weber, *J. Am. Chem. Soc.*, 1982, **104**, 5245.

11 A. S. Cherodian, A. N. Davies, R. M. Richardson, M. J. Cook, N. B. McKeown, A. J. Thomson, J. Feijoo, G. Ungar and K. J. Harrison, *Mol. Cryst. Liq. Cryst.*, 1991, **196**, 103; M. J. Cook, *J. Mater. Sci., Mater. Electron.*, 1994, **5**, 117; M. J. Cook, S. J. Cracknell and K. J. Harrison, *J. Mater. Chem.*, 1991, **1**, 703 and references therein..

12 N. B. McKeown, I. Chambrier and M. J. Cook, *J. Chem. Soc., Perkin Trans. 1*, 1990, 1169; I. Chambrier, M. J. Cook, S. J. Cracknell and J. McMurdo, *J. Mater. Chem.*, 1993, **3**, 841.

13 M. J. Cook, D. A. Mayes and R. H. Poynter, *J. Mater. Chem.*, 1995, **5**, 2233.

14 J. D. Wright, P. Roissin, G. P. Rigby, R. J. M. Nolte, M. J. Cook and S. C. Thorpe, *Sens. Actuators B*, 1993, **13–14**, 276.

15 C. Ometto, C. Fabris, C. Milanesi, G. Jori, M. J. Cook and D. A. Russell, *Br. J. Cancer*, 1996, **74**, 1891.

16 M. J. Cook, I. Chambrier, S. J. Cracknell, D. A. Mayes and D. A. Russell, *Photochem. Photobiol.*, 1995, **62**, 542.

17 A. McKillop and J. A. Tarbin, *Tetrahedron*, 1990, **31**, 5955.

18 R. Curci, A. Giovine and G. Modena, *Tetrahedron*, 1966, **22**, 1235; D. J. Brown and P. W. Ford, *J. Chem. Soc. (C)*, 1969, 2720; G. A. Russel and L. A. Ochrymowycz, *J. Org. Chem.*, 1970, **35**, 2106.

19 R. W. Murray and R. Jeyaraman, *J. Org. Chem.*, 1985, **50**, 2847; P. F. Corey and F. E. Ward, *J. Org. Chem.*, 1986, **51**, 1925; R. W. Murray, R. Jeyaraman and M. K. Pillay, *J. Org. Chem.*, 1987, **52**, 746; W. Adam, Y.-Y. Chan, D. Cremer, J. Gauss, D. Scheutzow and M. Schindler, *J. Org. Chem.*, 1987, **52**, 2800; W. Adam, W. Haas and G. Sieker, *J. Am. Chem. Soc.*, 1984, **106**, 5020.

20 Y. Miyahara and T. Inazu, *Tetrahedron Lett.*, 1990, **31**, 5955.

21 E. M. Maya, P. Haisch, P. Vazquez and T. Torres, *Tetrahedron*, 1998, **54**, 4397.

22 K. Poon, Y. Yan, X. Li and D. P. Ng, *Organometallics*, 1999, **18**, 3528; M. Hu, N. Brasseur, S. Z. Yildiz and J. E. van Lier, *J. Med. Chem.*, 1998, **41**, 1789.

23 M. J. Cook, S. J. Cracknell, G. R. Moore, M. J. Osborne and D. J. Williamson, *Magn. Reson. Chem.*, 1991, **29**, 1053.

24 E. Musluoglu, V. Ahsen, A. Gül and Ö. Bekâroglu, *Chem. Ber.*, 1991, **124**, 2531.

25 M. J. Cook, W. L. Davis and J. C. Swarts, unpublished work.

26 D. H. Evans, K. M. O' Connell, R. A. Peterson and M. J. Kelly, *J. Chem. Educ.*, 1983, **60**, 291; P. T. Kissinger and W. R. Heineman, *J. Chem. Educ.*, 1983, **60**, 702; J. J. van Benschoten, J. Y. Lewis and W. R. Heineman, *J. Chem. Educ.*, 1983, **60**, 772; T. Sawyer and J. L. Roberts Jr., *Experimental Electrochemistry for Chemists*, Wiley, New York, 1974, p. 118.

27 A. B. P. Lever, E. R. Milaeva and G. Speier in *Phthalocyanines: Properties and Applications*, eds. C. C. Leznoff and A. B. P. Lever, VCH, New York, 1993, vol. 3, pp. 1–69; R. H. Campbell, G. A. Heath, G. T. Hefter and R. C. S. McQueen, *J. Chem Soc., Chem. Commun.*, 1983, 1123.

28 D. W. Clack, N. S. Hush and I. S. Woolsey, *Inorg. Chim. Acta*, 1976, **19**, 129.

29 Y. L. Wong, J. F. Ma, W. F. Law, Y. Yan, W. T. Wong, Z. Y. Zhang, T. C. Mak and D. K. P. Ng, *Eur. J. Inorg. Chem.*, 1999, 313.

30 A. Giraudeau, A. Louati, M. Gross, J. J. Andre, J. Simon, C. H. Su and K. M. Kadish, *J. Am. Chem. Soc.*, 1983, **105**, 2917.

31 R. R. Gagne, C. A. Koval and G. C. Licensky, *Inorg. Chem.*, 1980, **19**, 2854.

32 Z. Jin, K. Nolan, C. R. McArthur, A. B. P. Lever and C. C. Leznof, *J. Organomet. Chem.*, 1994, **205**, 468; E. S. Schmidt, T. S. Calderwood and T. C. Bruice, *Inorg. Chem.*, 1986, **25**, 3718.

33 G. C. Bryant, M. J. Cook, C. Ruggiero, T. J. Ryan, A. J. Thorne, S. D. Haslam and R. M. Richardson, *Thin Solid Films*, 1994, **243**, 316.

34 D. T. Sawyer and J. L. Roberts Jr., *Experimental Electrochemistry for Chemists*, Wiley, New York, 1974, p. 54.

35 G. A. Mabbott, *J. Chem. Ed.*, 1983, **60**, 697.